

Synthesis and optical properties of benzocarbazole-substituted polysiloxanes for polymeric photorefractive materials

In Kyu Moon*, Jin-Woo Oh, Nakjoong Kim

Department of Chemistry, Hanyang University, Seoul 133-791, Republic of Korea

Received 31 May 2007; received in revised form 29 August 2007; accepted 31 August 2007

Available online 6 September 2007

Abstract

A novel polysiloxane having benzo[*a*]carbazole and benzo[*a,i*]carbazole pendant groups has been synthesized and characterized. We studied the electric-field-induced birefringence, the photoconductivity and the photorefractive (PR) properties of the polymeric PR composites. The PR composite showed a diffraction efficiency of 53% at 45 V/μm. A PR response time of 1.4 s at wavelength 633 nm was obtained, which was found to be higher than that of the carbazole-substituted polysiloxane composite.

© 2007 Elsevier B.V. All rights reserved.

Keywords: Benzocarbazole; Low glass temperature composite; Photorefractive effect

1. Introduction

Interest in the study of the PR effect has revived in the past 40 years, due mainly to the candidates for numerous applications, including high-density optical storage, dynamic holography, and optical image processing [1]. However, PR crystals have not become commercially feasible because they depend on the sensitivity of wavelength, are difficult and expensive to grow, and their properties cannot easily be modified. Among these materials, PR polymers have the potential to create a new range of material class and applications. Nowadays, most polymeric PR devices are composed of an poly(*N*-vinylcarbazole) (PVK)-based composites. In these composites, unstable device is crucial since electro-optic (EO) chromophore setting or aggregation affects its high stiffness. To overcome these disadvantages, an excess of plasticizers are often added to PVK to lower the glass transition temperature in PR system. We recently reported the synthesis and properties of the carbazole-substituted polysiloxane PR composites [2]. They have photoconductor properties similar to those of PVK but, in contrast to PVK, can be processed to create a flexible and stable device. However, a disadvantage of the carbazole-substituted polysiloxanes for use in PR was the

slow response time of grating formation of the four-wave mixing experimental.

For the further development of the carbazole-substituted side chain polymer as a hole transporter, studies on the polymers with various electron-donating units, e.g., triphenylamines, are helpful for a better understanding of the relationship between the chemical structures and chemical properties of the polymers. Among the electron-donating units, benzocarbazole derivatives are very attractive molecules due to their good hole-transporting ability [3]. However, in spite of the presence of a tremendous number of reports about PVK-based PR composite, the polymeric PR composite of a novel photoconductor-based has received less attention.

Along these lines, we report here the syntheses and characterization of benzocarbazole-substituted polysiloxanes. Also, we analyze PR performance of these glasses at a wavelength of $\lambda = 633$ nm when sensitized with C₆₀, and their photoconductivity and birefringence under external electric field.

2. Experimental

2.1. Materials and characterization

Toluene was distilled over sodium benzophenone under inert an argon atmosphere. Chloroform, dichloroethane, and DMF

* Corresponding author. Tel.: +82 2 2220 0935; fax: +82 2 2295 0572.
E-mail address: inkmoon@naver.com (I.K. Moon).

were dried by distillation over CaH_2 . The potassium hydroxide was quickly ground just before use when employed in the allylation reactions of benzocarbazole derivatives. All reagents and solvents were of commercial quality and were purified or dried and stored under nitrogen using standard procedures. All reactions were carried out under inert nitrogen or argon atmosphere. Monomer synthesis and polymerization were carried out as cited in Refs. [2,5,6]. The chemical structure of the new materials were characterized by ^1H NMR spectrometry (Varian, INOVA, 400 MHz), FT-IR spectrometry (Perkin-Elmer, Paragon 500), and UV–vis spectrometry (Duksan Mechasys, Optizen III). The glass transition temperature (T_g) of this composite was determined by differential scanning calorimetry (DSC, Perkin-Elmer DSC 7). The molecular weight and polydispersity were determined in THF solvent by a Waters GPC-410 calibrated with polystyrene standards.

2.2. Device preparation

In this work, low T_g PR material was prepared by doping the optically anisotropic chromophore, 2{3-[(*E*)-2-(piperidino)-1-ethenyl]-5,5-dimethyl-2-cyclohexenyliden}malono-nitrile (P-IP-DC) [2], into photoconducting polymer matrix, benzocarbazole-substituted polysiloxane sensitized by C_{60} as shown in Scheme 1. The composition of polymeric composite was polymer:P-IP-DC:BBP: C_{60} = 51:30:18:1 by wt%. The device was prepared by sandwiching the softened composite between two ITO coated glass plates. The thickness of active layer was 50 μm .

2.3. Measurement

All optical measurements were carried out at the composite's T_g . The EO property of the polymeric composite was determined by transmission ellipsometric method (632.8 nm, $I = 13 \text{ mW/cm}^2$). The sample tilted by 45° was placed between the polarizer and the analyzer with the polarization set to $+45^\circ$ and -45° , respectively. The Δn of composite was determined from the variation of the transmitted intensity (T) through crossed polarizers upon the application of electric field, as described by the following equation [2(b)]:

$$T = \sin^2 \left(\frac{2\pi}{\lambda} l \Delta n \right) \quad (1)$$

where λ is the wavelength and l is a distance of light path. The photoconductivity measurements ($\lambda = 632.8 \text{ nm}$) were performed on about 50 μm thick samples sandwiched between ITO electrodes at a $I = 13 \text{ mW/cm}^2$ using a photocurrent method [4]. The diffraction efficiency of PR material was determined by the degenerate four-wave mixing (DFWM) experiment. Two coherent laser beams at the wavelength of 632.8 nm were irradiated on the sample in the tilted geometry with the incident angle of 30° and 60° with respect to sample normal. The writing beams both were *s*-polarized and had the equal intensity of 60 mW/cm^2 . The recorded PR grating was read out by a *p*-polarized counter-propagating beam. Attenuated reading beam

with the very weak intensity of 0.1 mW/cm^2 was used. The internal diffraction efficiency (η_{int}) of PR material was determined from equation

$$\eta_{\text{int}} = \frac{I_{\text{R,diffracted}}}{I_{\text{R,diffracted}} + I_{\text{R,transmitted}}} \quad (2)$$

where $I_{\text{R,diffracted}}$ and $I_{\text{R,transmitted}}$ are the diffracted and transmitted intensities of reading beam, respectively.

2.4. Synthesis

Synthesis of 11-allyl-11H-benzo[a]carbazole. Yield: 75%. ^1H NMR (CDCl_3 , ppm) δ 4.81 (d, 1H), 5.05 (d, 1H), 5.21 (d, 2H), 5.97 (m, 1H), 7.30–8.77 (m, 10H).

Synthesis of 13-allyl-13H-benzo[a,i]carbazole. Yield: 63%. ^1H NMR (CDCl_3 , ppm) δ 5.30 (d, 1H), 5.59 (d, 1H), 5.50 (d, 2H), 6.78 (m, 1H), 7.54–8.57 (m, 12H).

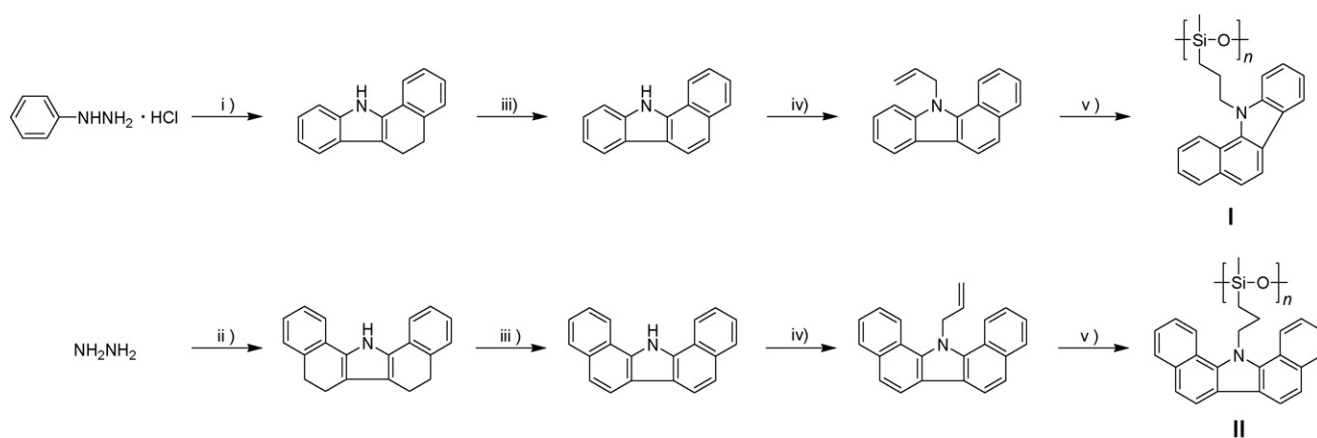
Synthesis of benzo[a]carbazole-substituted polysiloxane (polymer I). A solution of 11-allyl-11H-benzo[a]carbazole (2.99 g, 11.6 mol) and poly(methylhydro)siloxane (*ca.* $M_w = 2000$, 530 μl , 8.9 mmol) in toluene (50 ml) was stirred under argon atmosphere. Catalytic amount of hexachloroplatinate(IV)hydrate in propanol was added to the mixture. The mixture was stirred at elevated temperature (80°C) for 48 h. After cooling to ambient temperature, the mixture was poured onto methanol (500 ml). The precipitates were filtered off and dissolved in THF. The concentrated THF solution ($\sim 20 \text{ ml}$) was poured onto methanol (200 ml), and the precipitates were filtered off. The crude polymer **I** was purified by Soxhlet extraction with methanol for 2 days. Then the polymer **I** was again dissolved in the dry THF (60 ml). This THF solution was filtered through a ion-exchanged resin filter to remove residual catalyst particles and precipitated in methanol (600 ml). Residual solvent was evaporated under reduced pressure, and then the obtained polymer **I** was dried in a vacuum over at room temperature for 2 days. Yield: 69%. $T_g = 71^\circ\text{C}$. ^1H NMR (CDCl_3 , ppm) δ -1.80 to 2.00 (br m, 7H), 3.30–4.42 (br s, 2H), 6.70–7.93 (br t, 12H), 8.22 (br d, 2H).

Synthesis of benzo[a,i]carbazole-substituted polysiloxane (polymer II). The polymer **II** was prepared according to the method used for the polymer **I**. Yield: 64%. $T_g = 71^\circ\text{C}$. ^1H NMR (CDCl_3 , ppm) δ -0.26 to 0.49 (br s, 3H), 0.50–2.24 (br m, 4H), 5.12–5.42 (br s, 2H), 7.19–9.24 (br m, 12H).

3. Results and discussion

3.1. Synthesis and characterization

The preparation of polymers **I** and **II** was initiated by synthesis of monomer 11-allyl-11H-benzo[a]carbazole and 13-allyl-13H-dibenzo[a,i]carbazole depicted in Scheme 1. As can be seen in Scheme 1, the benzocarbazoles syntheses are of utility method of the Fisher indole syntheses. In the Fisher indole syntheses, the hydrazine molecules of ketone (α -tetralone) molecules is converted to substituted indole-derivatives by heating with an acid catalyst.



Scheme 1. Synthetic route of the monomers and the polymers. *Reaction conditions:* (i) α -tetralone, AcOH; (ii) α -tetralone, dry HCl, AcOH; (iii) Pd/C, Δ ; (iv) allyl bromide, KOH, DMF; (vi) poly(methylhydro)siloxane/hexachloroplatinate(IV)hydrate/toluene.

Dehydrogenation of 5,6-dihydro-11*H*-benzo[*a*]carbazole and 5,6,7,8-tetrahydro-13*H*-benzo[*a,i*]carbazole were heated at over 200 °C with palladium charcoal for several minutes. The 11*H*-benzo[*a*]carbazole and 13*H*-benzo[*a,i*]carbazole were obtained in good yield by simple thermolysis. Allylated-benzocarbazole derivatives were prepared in the presence of potassium hydroxide. The polymers **I** and **II** were prepared by hydrosilylation reaction using a platinum catalyst. The proceeding of the hydrosilylation was confirmed by disappearance of the signal at 4.8 ppm in the ^1H NMR spectrum and the peak at 2108 cm^{-1} of the starting Si–H in the IR spectrum. New peaks from methane (CH) and methylene (CH₂) protons in the polymer backbone appeared in the range of δ –1.80 to 2.24. They did not show peaks in the region of the resonance of allyl-group and Si–H. Aromatic protons were clearly observed in the ^1H NMR spectra as broad multiplets at aromatic regions.

Gel permeation chromatography using R.I. detection results from these polymerization reactions are reported in Table 1. The number average molecular weight, M_n , of polymers **I** and **II** determined by GPC versus a polystyrene standard were 4630 and 3520 with a P.D.I. (M_w/M_n) of 2.66 and 2.58, respectively. The glass transition temperatures (T_g) were also conducted on polymers **I** and **II** and revealed a low $T_g = 71$ and 64 °C, respectively.

Polymers **I** and **II** were good soluble in common organic solvents. Table 1 lists the absorption and photoluminescence (PL) maxima values. In films, polymers **I** and **II** showed strong UV–vis absorptions with λ_{max} at 295 and 297 nm, respectively, and only weak absorptions beyond 330 nm. These polymers present a broad and strong absorbance band like carbazole-

molecules in the UV–vis region. The $\lambda_{\text{max,PL}}$ values of the PL of the polymers **I** and **II** are at 377 and 394 nm (sh. 350 and 396 nm), and 423 nm (sh. 445 nm) in the solid state, indicating a blue emission.

3.2. Optical properties

The polymer composites consist of the polymer, EO chromophore, plasticizer butyl benzyl phthalate (BBP), and the sensitizer C₆₀. The composites are dissolved in 1,1,2,2-tetrachloroethane and evaporated to dryness. The composites are sandwiched between two patterned-ITO glass plates. After melting the composites at 110 °C for homogenous state, the polymer composites are rapidly cooled to avoid the crystallization (thickness = 50 μm). The resulting composite has a T_g of around 30 °C.

All optical experiments were performed at around T_g by illumination at a wavelength of 633 nm. The magnitude of the orientational birefringence of the PR polymer was characterized by transmission ellipsometric measurement at various applied fields [2b]. Since the orientational birefringence predominantly governs the steady-state PR property of low T_g polymer, this measurement enables us to assess the performance of chromophore. As given in Fig. 2(insert), the birefringence values (Δn) of the PR materials are increased quadratically with an electric field. The polymers **I** and **II** composites both exhibit the excellent electro-optic properties. This observation can be explained in terms of the dependence of dipole moment (μ) and polarizability anisotropy ($\Delta\alpha$) on a conjugation bridge [2]. The birefringence (Δn) of a composite containing the P-IP-DC

Table 1
Polymer characterization and spectroscopic data of the benzocarbazole-pendant polysiloxanes

	M_n^a (g/mol)	P.D.I. ^a (M_w/M_n)	λ_{abs}^b (nm)	λ_{PL}^b (nm)	T_g^c (°C)
Polymer I	4630	2.66	295, 330, 347	377, 394 [350, 396 (sh.)]	71
Polymer II	3520	2.58	297, 331, 347	423 [445 (sh.)]	64

^a M_n and polydispersity index (P.D.I.) of the polymers were determined by GPC using polystyrene standards.

^b In solid state (film).

^c T_g were determined by DSC at a scan rate of 10 °C/min.

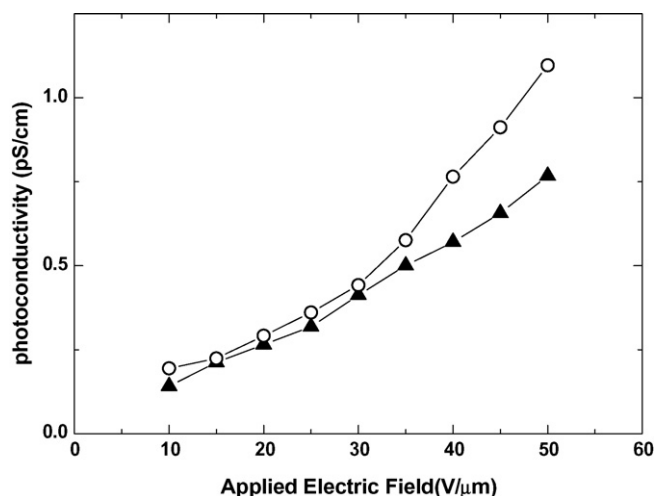


Fig. 1. Photoconductivity of the polymer **I** composite (open circle) and **II** composite (triangle) as a function of external electric field strength.

chromophore increased quadratically with increasing applied field. At an applied potential of 50 V/μm, ($I = 13 \text{ mW/cm}^2$), $\Delta n = 3.63 \times 10^{-3}$ for the polymer **I** composite and 3.45×10^{-3} for the polymer **II** composite, which are sufficiently large values for the preparation for efficient PR materials. The high electro-optic properties may be due to a large dipole moment as well as high polarizability anisotropy of P-IP-DC chromophore associated with the effective conjugation along the polyene type. Since the chromophores are rotating within an amorphous medium, they typically exhibit a non-exponential dynamic behavior.

The other important criterion for hole-transporting polymer design is to minimize its influence on photoconductivity, as mentioned above. The key factors that determine the process of the space-charge field formation are photoconductivity σ_{photo} , which has a complex characteristics combined with the effects of charge generation, charge mobility, and trapping. In order to determine the variation of photoconductivity by adding the P-IP-DC chromophore into benzocarbazole-pendant polysiloxane, photoconductivities of polymer composites were measured by simple dc method. As shown in Fig. 1, photoconductivity measurements of two samples yield photoconductivities σ_{photo} 1.10 pS/cm for the polymer **I** composite and 0.77 pS/cm for the polymer **II** composite at and applied electric field of 50 V/μm. This nonlinear dependence on the electric field is due to the electric field dependencies of both the quantum efficiency of charge generation and the mobility.

The internal diffraction efficiency (η_{int}) of the PR material was determined using the following equation:

$$\eta_{\text{int}} = \frac{I_{\text{R,diffracted}}}{I_{\text{R,diffracted}} + I_{\text{R,transmitted}}}$$

where $I_{\text{R,diffracted}}$ and $I_{\text{R,transmitted}}$ are the diffracted and transmitted intensities of the reading beam, respectively. The diffraction efficiency, η as a function of applied electric field, E , for each sample is shown in Fig. 2. At an external field of 50 V/μm at T_g ; ($I = 40 \text{ mW/cm}^2$), the values of the maximum diffraction efficiency (η_{max}) of the polymers **I** and **II** was 53% (at $E = 45 \text{ V/μm}$) and 39% (at $E = 40 \text{ V/μm}$). When the steady-state performance

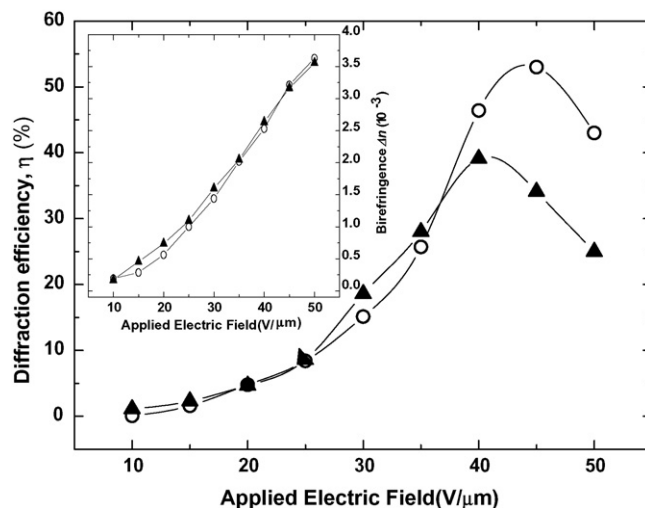


Fig. 2. Steady-state diffraction efficiency of the polymer **I** composite (open circle) and **II** composite (triangle) under vs. applied electric fields. The insert shows the electric-field-induced birefringence of the polymer **I** composite (open circle) and **II** composite (triangle) vs. applied fields.

of the PR materials is evaluated, $E(\eta_{\text{max}})$ can be used for a parameter: $E(\eta_{\text{max}})$ is decreased with the improvement of the PR property of the material [7]. The low value of $E(\eta_{\text{max}})$ shown in Fig. 2 proved the high performance of the polymer composite containing P-IP-DC chromophore, together with the high gain coefficient.

One of the major properties of PR composites has been the response time of the diffraction efficiency. This parameter is very important for real applications such as real imaging and real-data processing. To investigate the fast response time of PR devices, we measured the temperature dependence of the response time of the diffraction efficiency. The temperature dependences of the response time of the diffraction efficiencies are shown in Fig. 3. After 200 s, the other writing beam was applied and the diffracted reading beam was monitored. Time constants τ were calculated by fitting the evolution of the growth of the diffraction signal,

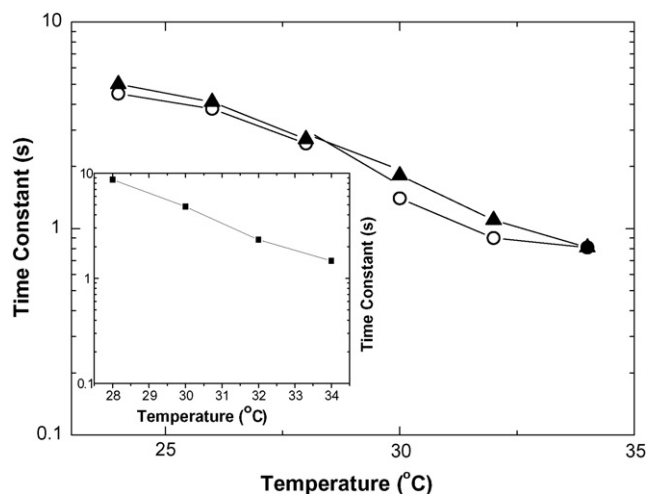


Fig. 3. Temperature dependences of the response time of the diffraction efficiencies: polymer **I** composite (open circle) and **II** composite (triangle). The insert shows the response time of PSX-Cz composite [2] vs. temperature.

Table 2
Composition of the investigated composites and some photo-physical properties

Composites	σ_{photo}^a (pS/cm)	Δn^b ($\times 10^{-3}$)	η (%)	τ^c (s)
Composite I	1.10	3.63	53 ^d	1.4
Composite II	0.77	3.45	39 ^e	1.8

^a Taken at $E = 50$ V/ μm .

^b Taken at $E = 50$ V/ μm .

^c Taken at $T = 30^\circ\text{C}$.

^d Taken at $E = 45$ V/ μm .

^e Taken at $E = 40$ V/ μm .

$\eta(t)$ [8]. The response time of diffraction efficiency becomes larger as the temperature rises above the polymer composite's T_g . The change in temperature had the largest avail of a PR speed. This behavior is thought to originate from the differences in both the reorientation speed and the photoconductivity. As the temperature increase above T_g , the orientational speed also increases. In low T_g systems, the orientation mobility of the P-IP-DC dye molecules increases, resulting in a enlarged orientational enhancement contribution to the grating amplitude. We obtained exhibit the response time of 1.4 s for the polymer **I** composite and 1.8 s for the polymer **II** composite under 30°C . It is found that the PR response rate of these composites is faster than that of the carbazole-substituted polysiloxane composite (see Fig. 3(insert)) [2]. This composite was based on photoconducting carbazole-substituted polysiloxane (PSX-Cz) doped 2-{3-[(*E*)-2(dibutylamino)-1-ethenyl]-5,5-dimethyl-2-cyclohexenyliden} malononitrile (DB-IP-DC) chromophore and 2,4,7-trinitro-9-fluorenone (TNF). The composition of the sample was PSX-Cz:DB-IP-DC:TNF at a ratio of 69:30:1 wt%. The PSX-Cz composite showed a T_g of 27°C without any extra plasticizer. At higher temperatures, the film is softened and can be polarized readily by the external electric field and a large electro-optic effect can be induced. In addition, the P-IP-DC dye becomes more mobile. However, the diffraction efficiency of the polymer **I** composite and **II** composite is lower that of the PSX-Cz composite (92% at $E = 30$ V/ μm). This behavior is

probably due to lower trap. The PR response rate and diffraction efficiency of the polymer **I** composite and **II** composite are listed in Table 2.

4. Conclusion

Here we presented benzocarbazole-substituted polysiloxanes, polymers **I** and **II**, for PR materials. The polymer composites containing these chromophores exhibited the excellent birefringence, photoconductivity, and photorefractive properties.

The polymer **I** composite showed a diffraction efficiency of 53% at 45 V/ μm , which corresponded to a Δn of 3.63×10^{-3} . Also, this composite shows the PR response time of 1.4 s at 30°C . The PR response time and diffraction efficiency of the present devices, however, require much further improvement to be acceptable for practical application.

Acknowledgements

This research has been made possible by the financial support of Korea CRI Program. The authors also thank Mr. C.-S. Choi for assistance with the optical measurements.

References

- [1] A. Ashkin, G.D. Boyd, J.M. Dziedzic, R.G. Smith, A.A. Ballmann, H.J. Levinstein, K. Nassau, Appl. Phys. Lett. 9 (1966) 72.
- [2] (a) H. Chun, I.K. Moon, D.-H. Shin, N. Kim, Chem. Mater. 13 (2001) 2813; (b) H. Chun, I.K. Moon, D.-H. Shin, S. Song, N. Kim, J. Mater. Chem. 12 (2002) 858.
- [3] E.L. Aleksandrova, Semiconductors 38 (2004) 1115.
- [4] J.S. Schildkraut, Appl. Phys. Lett. 58 (1991) 340.
- [5] P. Strohmriegel, Makromol. Chem. Rapid Commun. 771 (1986) 7.
- [6] A.R. Katrizky, Z. Wang, J. Heterocycl. Chem. 25 (1998) 671.
- [7] R. Bittner, T.K. Daubler, D. Neher, K. Meerholz, Adv. Mater. 11 (1999) 123.
- [8] G. Bauml, S. Schoter, U. Hofmann, D. Haarer, Opt. Commun. 75 (1998) 154.